J. Math. Anal. Appl. 382 (2011) 34–46

Contents lists available at ScienceDirect

Journal of Mathematical Analysis and Applications

www.elsevier.com/locate/jmaa

An innovative multistage, physiologically structured, population model to understand the European grapevine moth dynamics

Bedr'eddine Ainseba [a], Delphine Picart [b,*], Denis Thiéry [c]

[a] Bordeaux University, IMB UMR CNRS 5251, Anubis Team INRIA Bordeaux Sud Ouest, 3 Ter Place de La Victoire Batiment Leyteire, 33076 Bordeaux Cedex, France
[b] Arizona State University, School of Mathematical and Statistical Sciences, Tempe, AZ 85287-1804, United States
[c] UMR 1065 INRA-ENITAB en Santé Végétale, Institut des Sciences de la Vigne et du Vin, centre de recherches de Bordeaux, B.P.81, F-33883 Villenave d'Ornon Cedex, France

ARTICLE INFO

Article history:
Received 8 September 2010
Available online 15 April 2011
Submitted by J. Shi

Keywords:
Population dynamics
Age-structured population model
Partial differential equations
Grape variety
Hyperbolic system

ABSTRACT

We present a multistage, physiologically structured, population model for studying the dynamics of one of the most important grapevine insect pests. Growth of the population at each stage is modeled considering the climatic variations and the grape variety. A result of existence and uniqueness of solutions is presented for this original hyperbolic system as well as simulations of experimental field data.

1. Introduction

Lobesia botrana, the European grapevine moth (EGVM), is a grape pest causing important economic damages [20]. Not only does it reduce the number of fruits, especially in spring when buds are flowering or berries are young, but also affecting their quality by favoring indirect damages related to different pathogens developing on the fruits, such as the grey mold or, in several warm vineyards, the black rots that may produce fungi toxins like ochratoxins [20]. Several families of pesticides are used to decrease the population size of the moth, but serious environmental damages can ensue from their use. Such phytosanitary problems could become more prevalent in the future due to climatic changes. Currently, the control procedures for this pest rely mainly on larval growth regulators, slightly on mating disruption (no more than 2% of the French wine areas in 2007) and scarcely on Bt toxin in sprays. One problem concerning these control techniques is that their efficiency depends upon the timing of the treatment and its synchrony with a few specific steps of the pest life cycle such as adult flight and oviposition periods. Therefore, population dynamic models should prove to be very helpful to determine an optimal window of time in the life history cycle. Researchers are developing some tools to control these insect populations and also to reduce the application of chemical plant health products. Their goal is to predict the periods of appearance of the insect in the vineyard, and mathematical models may help achieve this objective.

Like in many insects, the life cycle of the EGVM can be divided into four developmental stages, which are egg, larva, pupa and moth. The first three stages correspond to the insect growth and the last stage to adulthood. This life cycle is repeated two to five times per year depending on the vineyard latitude [20]. As a function of temperature and food availability, this cycle lasts about two months during spring and less in summer, with a critical minimum duration of one month for a complete generation. The winter generation diapauses as a pupa and lasts circa six months. We are interested, in this

---

[*] Corresponding author.
E-mail addresses: bedreddine.ainseba@u-bordeaux2.fr (B. Ainseba), delphinepicart@hotmail.com (D. Picart), thiery@bordeaux.inra.fr (D. Thiéry).

0022-247X/$ – see front matter
doi:10.1016/j.jmaa.2011.04.021

paper, in the spring and summer generations where the pupa stage lasts one week, and we assume that the pupal stage is included in the larval stage to form a single stage, the larval stage.

The developmental time of each growth stage varies with the individual, but also as a result of environmental variables and resource quality and availability. The major factor that affects the insect growth is temperature, but others may also contribute favorably or negatively to the individual growth and to the population size. Experimental data obtained on field populations and in various geographical areas shows the effect of the moisture factor [1,6,15]. It contributes to accelerate or slow down the insect growth and, for specific values, to drastically increase the mortality of the offspring. Food quality, especially grape variety consumed by the larva, affects several life history traits related to the reproductive success [10,11, 13,19]. Thus, the climatic and environmental variables considered here are temperature, moisture, and grape variety as a provider differential food quality to the growing larval instars. The competition for food between larvae is also modeled because it plays a role in the mortality rate. Other factors, such as predation, affect the population dynamics of this insect through the mortality rate. We have neglected these factors in this study and focus on the modeling of the natural development of several cohorts of this insect.

Since 1979, several models have been developed to predict the population "peaks" of this insect in vineyards [3,4,22]. These models, which are ordinary differential equations or discrete equations, describe the period and the length of the spring and summer population dynamics for egg, larval and adult stages. The temperature is the only environmental factor implicated to predict the population size in time as a growth factor. As a consequence, other relevant aspects of the dynamics, for example the mortality or inter-cohort growth variations, are missing and the predictions are not satisfying.

In the literature, Partial Differential Equations (PDEs) are also used to describe the dynamics of a single population [14]. These equations enable us to model physiological characteristics such as age or size to differentiate individuals within a cohort. For example, Sinko and Streifer's model is the well-known model used in the study of age-size structured populations [5,18].

To explore the importance of growth variations within a cohort, we propose to model the EGVM population dynamics by a stage-structured population model based on PDEs. This article is then built as follows: In Section 2 we present the model called *Lobesia botrana* model (LBM) and we provide a proof of existence and uniqueness of its solution based on fixed point theory. In Section 3, we show some simulations of LBM and compare them with field experimental data.

2. The *Lobesia botrana* model and its well-posedness

To properly describe the reproductive cycle of the EGVM, we consider a multistage, physiologically structured, population model. We denote by u^e, u^l, u^m, and u^f, respectively, the age density distribution at time t of egg, larva, male and female populations. The total population for the k-stage is then defined by

$$P^k(t) = \int_0^{L^k} u^k(t,a)\,da, \quad t \geqslant 0,$$

where L^k is the maximum age for the k-stage, and k takes the value e for egg, l for larva, m for male and f for female. The model describing the dynamics of these populations reads

$$\begin{cases} \dfrac{\partial}{\partial t}u^e(t,a) + \dfrac{\partial}{\partial a}\big[v^e\big(E(t),a\big)u^e(t,a)\big] = -m^e\big(E(t),a\big)u^e(t,a) - \beta^e\big(E(t),a\big)u^e(t,a), \\ \dfrac{\partial}{\partial t}u^l(t,a) + \dfrac{\partial}{\partial a}\big[v^l\big(E(t),a\big)u^l(t,a)\big] = -m^l\big(P^l(t),E(t),a\big)u^l(t,a) - \beta^l\big(E(t),a\big)u^l(t,a), \\ \dfrac{\partial}{\partial t}u^f(t,a) + \dfrac{\partial}{\partial a}\big[v^f\big(E(t),a\big)u^f(t,a)\big] = -m^f\big(E(t),a\big)u^f(t,a), \\ \dfrac{\partial}{\partial t}u^m(t,a) + \dfrac{\partial}{\partial a}\big[v^m\big(E(t),a\big)u^m(t,a)\big] = -m^m\big(E(t),a\big)u^m(t,a), \end{cases} \tag{2.1}$$

where the time variable t is defined on $[0,T]$ and the age variable a is given on $[0,L^k]$, $k=e,l,f,m$. We denote by Ω^k the domain $[0,T]\times[0,L^k]$, $k=e,l,f,m$.

The vector $E=(T,H,R)$ corresponds to the climatic and environmental factors where T is the temperature factor, H the humidity factor and R the grape variety factor. The vector E is time-dependent. We stress that R is not the quantity of food eaten by the larva but rather depends on the species of the vine.

The functions m^k, $k=e,l,f,m$, are the k-stage age-specific per capita mortality functions. To model the inter-individual competition between larvae for food, we assume that m^l depends on the total larvae population.

The functions β^k, $k=e,l$, correspond to the k-stage age-specific transition functions. In particular, β^e-called the hatching function-models the physiological change between egg and larval stages. The emerging adult function β^l is the transition between the larval and moth stages. The transition function between the moth and egg stages is modeled by the function β^f. The common name is the age-specific per capita birth function. Observations on EGVM indicate that the population does not grow exponentially but reaches a threshold value determined by the carrying capacity of the food. One bunch can hardly house more than 15 larvae depending upon the bunch size [19]. The growth of the population size is not restricted by the food quantity but by the total number of moths per unit of volume. Therefore, the birth function is dependent on the density of individuals.

The study of laboratory data shows a difference in growth between individuals assembled in cohorts [1,10,11]. This phenomenon is classical and has been observed for many other species. Mathematicians often model growth variability by introducing growth function that depends on the physiological age [5]. In LBM, functions v^k, $k = e, l, f, m$, represent the k-stage age-specific per capita growth functions. These functions are age-dependent and, coupled with the transition functions, allow us to model great variability of growth within a cohort.

The set of demographic functions (m^k, v^k, β^e, β^l, β^f), $k = e, l, f, m$, vary with the climatic and environmental factors E.

The boundary conditions related to (2.1) are defined in (2.2),

$$\begin{cases} v^e\big(E(t),0\big)u^e(t,0) = \displaystyle\int_0^{L^f} \beta^f\big(P^f(t), P^m(t), E(t), s\big)u^f(t,s)\,ds, \\ v^l\big(E(t),0\big)u^l(t,0) = \displaystyle\int_0^{L^e} \beta^e\big(E(t), s\big)u^e(t,s)\,ds, \\ v^f\big(E(t),0\big)u^f(t,0) = \displaystyle\int_0^{L^l} \tau\beta^l\big(E(t), s\big)u^l(t,s)\,ds, \\ v^m\big(E(t),0\big)u^m(t,0) = \displaystyle\int_0^{L^l} (1-\tau)\beta^l\big(E(t), s\big)u^l(t,s)\,ds, \end{cases} \tag{2.2}$$

where τ denotes the sex-ratio and $t > 0$; the initial conditions are given in (2.3),

$$u^k(0,a) = u_0^k(a), \quad a \in \big[0, L^k\big],\ k = e, l, f, m. \tag{2.3}$$

The equations in (2.2) model, respectively, the total number of new eggs, larvae, female and male moths at time t. Note that the integral over an age range of the product $v^k u^k$, $k = e, l, f, m$, does not represent in this model a number of individuals at the corresponding time. Indeed, in similar models we have, for example, a size structured population model [5,7,18] where this integral represents the total biomass of the population at time t. For the model (2.1), this integral has no clear biological meaning, except that it represents some measure of the "total maturity" of the population at time t.

Many population models using PDEs are used to describe a whole population instead sub-populations as LBM does. Although the equations related to adult stages of (2.1) look like Sinko and Streifer's model from a mathematical point of view, the first two equations are not equivalent to their population models because of the additional terms modeling the proportion of individuals who change physiological state. Moreover, the additional terms of the egg and larval equations are also the boundary conditions of the larval and adult stages respectively. Therefore, all equations in our system are dependent from each other, making the mathematical analysis more complicated. Finally, even though there exist many species with a similar life cycle to that of EGVM, LBM does not exist in the literature. Also, because of its original form, LBM enables us to study new mathematical and biological questions.

2.1. Existence and uniqueness

In this subsection, we are looking for the well-posedness of the mathematical model (2.1)–(2.3).

First, we define the functions h^k, for $k = e, l, f, m$, by

$$\begin{cases} h^e(t,a) = \big(m^e + \beta^e + \partial_a v^e\big)\big(E(t), a\big), \\ h^l(t,a) = m^l\big(P^l(t), E(t), a\big) + \big(\beta^l + \partial_a v^l\big)\big(E(t), a\big), \\ h^f(t,a) = \big(m^f + \partial_a v^f\big)\big(E(t), a\big), \\ h^m(t,a) = \big(m^m + \partial_a v^m\big)\big(E(t), a\big), \end{cases}$$

where $\partial_a v^k$ denotes the first derivative of the function v^k with respect to the age variable. Then, using the method of characteristics (see, for example, [2] for an introduction to the method) we get the following implicit equations for the densities u^e, u^l, u^f and u^m,

$$u^k(t,a) = \begin{cases} u_0^k(X^k(0;t,a))e^{-\int_0^t h^k(s,X^k(s;t,a))\,ds}, & a > X^k(t), \\ \frac{u^k(Z^k(0;t,a),0)}{v^k(E(Z^k(0;t,a)),0)} e^{-\int_{Z^k(0;t,a)}^t h^k(s,X^k(s;t,a))\,ds}, & a \leqslant X^k(t), \end{cases} \tag{2.4}$$

for $k = e, l, f, m$, where $X^k(t; t, a)$ and $Z^k(a; t, a)$ are the characteristic curves for the k-stage equation, passing through the point (t, a) and satisfying, respectively, these initial value problems:

$$\begin{cases} (X^k)'(t) = v^k(E(t), X^k(t)), \\ X^k(0) = 0, \end{cases} \tag{2.5}$$

for the time-dependent characteristic curve and

$$\begin{cases} (Z^k)'(a) = v^k(E(Z^k(a)), a), \\ Z^k(0) = 0, \end{cases} \tag{2.6}$$

for the characteristic curve expressed in the age variable. The existence of these solutions depends on the properties of the demographic functions and initial conditions. We then define the following assumptions.

H1. The growth functions v^k, for $k = e, l, f, m$, are bounded, non-negative functions at age 0:

$$0 < \underline{v^k} < v^k(E(t), 0) < \overline{v^k}, \quad \forall t \in [0, T],$$

and continuously differentiable with respect to the age variable:

$$\left\| \frac{\partial v^k(E(t), a)}{\partial a} \right\|_\infty \leqslant C_{v^k}, \quad \forall (t, a) \in \Omega^k,$$

where C_{v^k} are positive constants.

H2. The hatching function $\beta^e(E(t), a)$ and the flying function $\beta^l(E(t), a)$ are bounded, and non-negative functions with respect to the age variable.

H3. The birth function $\beta^f(P^f, E(t), a)$ is bounded, non-negative with respect to the age variable, and is Lipschitz with constant β_K^f with respect to the first variable P^f.

H4. The mortality functions $m^e(E(t), a)$, $m^f(E(t), a)$ and $m^m(E(t), a)$ are non-negative, locally bounded, and satisfy the conditions

$$\lim_{a \to L^k} \int_0^t m^k(E(t), X^k(s; t, a))\, ds = \infty, \quad a > X^k(t),$$

$$\lim_{a \to L^k} \int_{Z^k(0;t,a)}^t m^k(E(t), X^k(s; t, a))\, ds = \infty, \quad a \leqslant X^k(t),$$

for $t > 0$ and $k = e, f, m$. The functions X^k and Z^k are the characteristic curves defined in (2.5) and (2.6).

H5. The mortality function of the larva stage, $m^l(P^l, E(t), a)$, is non-negative, locally bounded, Lipschitz with respect to the first variable, and satisfies the conditions

$$\lim_{a \to L^l} \int_0^t m^l(P^l(t), E(t), X^l(s; t, a))\, ds = \infty, \quad a > X^l(t),$$

$$\lim_{a \to L^l} \int_{Z^l(0;t,a)}^t m^l(P^l(t), E(t), X^l(s; t, a))\, ds = \infty, \quad a \leqslant X^l(t),$$

for $t > 0$. The functions X^l and Z^l are the characteristic curves defined in (2.5) and (2.6).

H6. The initial functions u_0^k, for $k = e, l, f, m$ are non-negative.

As the solutions u^e, u^l, u^f and u^m exist under the previous hypothesis, we are looking for their uniqueness. According to Eq. (2.4), the four density functions are linked through their boundary conditions. Indeed, the density of the egg population, u^e, is expressed by the number of newborns laid by all the females. The densities describing the adult stages, u^f and u^m are dependent on the larval density u^l, whereas this last is dependent on the egg density u^e. To overcome this difficulty in our result of uniqueness, we propose to modify our model so that we can apply a fixed point argument to reach our goal. Theorem 1 and its proof present this result.

Theorem 1. *Under the hypotheses* (H1)–(H6)*, the system* (2.1)–(2.3) *admits a unique solution.*

Proof. Let λ be a positive constant and introduce the following variables

$$u^k(t,a)=e^{\lambda t}\hat{u}^k(t,a),\quad k=e,l,f,m. \tag{2.7}$$

Using (2.7), the system (2.1)–(2.3) is then transformed into system (2.8)

$$\begin{cases}
\dfrac{\partial}{\partial t}\hat{u}^e(t,a)+\dfrac{\partial}{\partial a}\big[v^e\big(E(t),a\big)\hat{u}^e(t,a)\big]+\lambda\hat{u}^e(t,a)=-m^e\big(E(t),a\big)\hat{u}^e(t,a)-\beta^e\big(E(t),a\big)\hat{u}^e(t,a),\\
\dfrac{\partial}{\partial t}\hat{u}^l(t,a)+\dfrac{\partial}{\partial a}\big[v^l\big(E(t),a\big)\hat{u}^l(t,a)\big]+\lambda\hat{u}^l(t,a)=-m^l\big(P^l,E(t),a\big)\hat{u}^l(t,a)-\beta^l\big(E(t),a\big)\hat{u}^l(t,a),\\
\dfrac{\partial}{\partial t}\hat{u}^f(t,a)+\dfrac{\partial}{\partial a}\big[v^f\big(E(t),a\big)\hat{u}^f(t,a)\big]+\lambda\hat{u}^f(t,a)=-m^f\big(E(t),a\big)\hat{u}^f(t,a),\\
\dfrac{\partial}{\partial t}\hat{u}^m(t,a)+\dfrac{\partial}{\partial a}\big[v^m\big(E(t),a\big)\hat{u}^m(t,a)\big]+\lambda\hat{u}^m(t,a)=-m^m\big(E(t),a\big)\hat{u}^m(t,a),\\
v^e\big(E(t),0\big)\hat{u}^e(t,0)=\displaystyle\int_0^{L^f}\beta^f\big(P^f(t),E(t),s\big)\hat{u}^f(t,s)\,ds,\\
v^l\big(E(t),0\big)\hat{u}^l(t,0)=\displaystyle\int_0^{L^e}\beta^e\big(E(t),s\big)\hat{u}^e(t,s)\,ds,\\
v^f\big(E(t),0\big)\hat{u}^f(t,0)=\tau\displaystyle\int_0^{L^l}\beta^l\big(E(t),s\big)\hat{u}^l(t,s)\,ds,\\
v^m\big(E(t),0\big)\hat{u}^m(t,0)=(1-\tau)\displaystyle\int_0^{L^l}\beta^l\big(E(t),s\big)\hat{u}^l(t,s)\,ds,\\
\hat{u}^k(0,a)=\hat{u}_0^k(a),\quad k=e,l,f,m,
\end{cases} \tag{2.8}$$

which admits a solution under the hypotheses (H1)–(H6). Now, we consider the following system

$$\begin{cases}
\dfrac{\partial}{\partial t}\hat{u}^e(t,a)+\dfrac{\partial}{\partial a}\big[v^e\big(E(t),a\big)\hat{u}^e(t,a)\big]+\lambda\hat{u}^e(t,a)=-m^e\big(E(t),a\big)\hat{u}^e(t,a)-\beta^e\big(E(t),a\big)\hat{u}^e(t,a),\\
\dfrac{\partial}{\partial t}\hat{u}^l(t,a)+\dfrac{\partial}{\partial a}\big[v^l\big(E(t),a\big)\hat{u}^l(t,a)\big]+\lambda\hat{u}^l(t,a)=-m^l\big(P^l_\phi,E(t),a\big)\hat{u}^l(t,a)-\beta^l\big(E(t),a\big)\hat{u}^l(t,a),\\
\dfrac{\partial}{\partial t}\hat{u}^f(t,a)+\dfrac{\partial}{\partial a}\big[v^f\big(E(t),a\big)\hat{u}^f(t,a)\big]+\lambda\hat{u}^f(t,a)=-m^f\big(E(t),a\big)\hat{u}^f(t,a),\\
\dfrac{\partial}{\partial t}\hat{u}^m(t,a)+\dfrac{\partial}{\partial a}\big[v^m\big(E(t),a\big)\hat{u}^m(t,a)\big]+\lambda\hat{u}^m(t,a)=-m^m\big(E(t),a\big)\hat{u}^m(t,a),\\
v^e\big(E(t),0\big)\hat{u}^e(t,0)=\displaystyle\int_0^{L^f}\beta^f\big(P^f_\phi(t),E(t),s\big)\hat{u}^f(t,s)\,ds,\\
v^l\big(E(t),0\big)\hat{u}^l(t,0)=\displaystyle\int_0^{L^e}\beta^e\big(E(t),s\big)\hat{u}^e(t,s)\,ds,\\
v^f\big(E(t),0\big)\hat{u}^f(t,0)=\tau\displaystyle\int_0^{L^l}\beta^l\big(E(t),s\big)\phi(t,s)\,ds,\\
v^m\big(E(t),0\big)\hat{u}^m(t,0)=(1-\tau)\displaystyle\int_0^{L^l}\beta^l\big(E(t),s\big)\phi(t,s)\,ds,\\
\hat{u}^k(0,a)=\hat{u}_0^k(a),\quad k=e,l,f,m,
\end{cases} \tag{2.9}$$

where ϕ is a function in $L^2(\Omega^l)$. From this last system (2.9), we get a uniqueness result that is summarized in Lemma 1.

Lemma 1. *Let* (H1)–(H6) *be satisfied and* $\wedge$ *be the operator defined by*

$$\begin{aligned}&\wedge : L^2(\Omega^l) \to L^2(\Omega^l),\\ &\qquad \phi \to \hat{u}^l\end{aligned}\tag{2.10}$$

where $\hat{u}^l$ *is the unique solution of* (2.9). *If* λ *satisfies the condition*

$$\left(\lambda - C_{v^l} - \frac{\|\hat{u}_2^l\|^2_{L^\infty}}{2\epsilon}\right)(\lambda - C_{v^e})(\lambda - C_{v^f}) > \left(D + (\lambda - C_{v^e})(\lambda - C_{v^f})\frac{\epsilon}{2}\left(m_N^l L^l\right)^2\right),$$

for some positive constants ϵ *and* D, *then* $\wedge$ *is contractive.*

Assuming that Lemma 1 is true, the operator $\wedge$ defined in (2.10) has a fixed point that will be named $\hat{u}^l$, which is the unique solution of (2.9). This last result also proves that the density $\hat{u}^l$ is the unique solution of (2.8) and, by using the change of variables given in (2.7), that the density u^l is the unique solution of our initial problem (2.1)–(2.3). Eq. (2.4) then gives us the unique existence of densities u^e, u^f and u^m, concluding the proof of Theorem 1. □

Proof of Lemma 1. Let ϕ_i, for $i = 1, 2$, be two functions satisfying system (2.9). And let $\phi = \phi^1 - \phi^2$, $\hat{u}^l = \hat{u}_1^l - \hat{u}_2^l$, $\hat{u}^e = \hat{u}_1^e - \hat{u}_2^e$, $\hat{u}^f = \hat{u}_1^f - \hat{u}_2^f$ and $\hat{u}^m = \hat{u}_1^m - \hat{u}_2^m$. We multiply the first equation of system (2.9) by $\hat{u}^e$, the second by $\hat{u}^l$, the third by $\hat{u}^f$ and the fourth by $\hat{u}^m$ to obtain

$$\begin{cases}\dfrac{1}{2}\dfrac{\partial}{\partial t}\left(\hat{u}^e(t,a)\right)^2 + \hat{u}^e(t,a)\dfrac{\partial}{\partial a}\left[v^e\left(E(t),a\right)\hat{u}^e(t,a)\right] + \lambda\left(\hat{u}^e(t,a)\right)^2 = -\left(m^e\left(E(t),a\right) + \beta^e\left(E(t),a\right)\right)\left(\hat{u}^e(t,a)\right)^2,\\[2mm] \dfrac{1}{2}\dfrac{\partial}{\partial t}\left(\hat{u}^l(t,a)\right)^2 + \hat{u}^l(t,a)\dfrac{\partial}{\partial a}\left[v^l\left(E(t),a\right)\hat{u}^l(t,a)\right] + \lambda\left(\hat{u}^l(t,a)\right)^2 = -\left(m^l\left(P^l_\phi, E(t),a\right) + \beta^l\left(E(t),a\right)\right)\left(\hat{u}^l(t,a)\right)^2,\\[2mm] \dfrac{1}{2}\dfrac{\partial}{\partial t}\left(\hat{u}^f(t,a)\right)^2 + \hat{u}^f(t,a)\dfrac{\partial}{\partial a}\left[v^f\left(E(t),a\right)\hat{u}^f(t,a)\right] + \lambda\left(\hat{u}^f(t,a)\right)^2 = -m^f\left(E(t),a\right)\left(\hat{u}^f(t,a)\right)^2,\\[2mm] \dfrac{1}{2}\dfrac{\partial}{\partial t}\left(\hat{u}^m(t,a)\right)^2 + \hat{u}^m(t,a)\dfrac{\partial}{\partial a}\left[v^m\left(E(t),a\right)\hat{u}^m(t,a)\right] + \lambda\left(\hat{u}^m(t,a)\right)^2 = -m^m\left(E(t),a\right)\left(\hat{u}^m(t,a)\right)^2.\end{cases}$$

These last equations are then integrated, respectively, on the domains Ω^e, Ω^l, Ω^f, Ω^m, to get after some computations the following system,

$$\int_{\Omega^e}\left(\lambda + m^e\left(E(t),a\right) + \beta^e\left(E(t),a\right) + \frac{1}{2}\partial_a v^e\left(E(t),a\right)\right)\left(\hat{u}^e(t,a)\right)^2\,da\,dt = \frac{1}{2}\int_0^T v^e\left(E(t),0\right)\left(\hat{u}^e(t,0)\right)^2\,dt,$$

$$\begin{aligned}&\int_{\Omega^l}\left(\lambda + m^l\left(P^l_{\phi_1}(t), E(t),a\right) + \beta^l\left(E(t),a\right) + \frac{1}{2}\partial_a v^l\left(E(t),a\right)\right)\left(\hat{u}^l(t,a)\right)^2\,da\,dt\\ &\quad = -\int_{\Omega^l}\left(m^l\left(P^l_{\phi_1}(t), E(t),a\right) - m^l\left(P^l_{\phi_2}(t), E(t),a\right)\right)\hat{u}_2^l(t,a)\hat{u}^l(t,a)\,da\,dt + \frac{1}{2}\int_0^T v^l\left(E(t),0\right)\left(\hat{u}^l(t,0)\right)^2\,dt,\end{aligned}$$

$$\int_{\Omega^f}\left(\lambda + m^f\left(E(t),a\right) + \frac{1}{2}\partial_a v^f\left(E(t),a\right)\right)\left(\hat{u}^f(t,a)\right)^2\,da\,dt = \frac{1}{2}\int_0^T v^f\left(E(t),0\right)\left(\hat{u}^f(t,0)\right)^2\,dt,$$

$$\int_{\Omega^m}\left(\lambda + m^m\left(E(t),a\right) + \frac{1}{2}\partial_a v^m\left(E(t),a\right)\right)\left(\hat{u}^m(t,a)\right)^2\,da\,dt = \frac{1}{2}\int_0^T v^m\left(E(t),0\right)\left(\hat{u}^m(t,0)\right)^2\,dt.$$

These last equations become inequalities (2.11) using hypotheses (H1)–(H6).

$$\begin{cases} (\lambda - C_{\nu^e}) \displaystyle\int_{\Omega^e} \big(\hat{u}^e(t,a)\big)^2 \, da\, dt \leqslant \frac{1}{2} \int_0^T \nu^e\big(E(t),0\big)\big(\hat{u}^e(t,0)\big)^2 \, dt, \\ (\lambda - C_{\nu^l}) \displaystyle\int_{\Omega^l} \big(\hat{u}^l(t,a)\big)^2 \, da\, dt \leqslant \frac{1}{2} \int_0^T \nu^l\big(E(t),0\big)\big(\hat{u}^l(t,0)\big)^2 \, dt \\ \qquad\qquad - \displaystyle\int_{\Omega^l} \big(m^l\big(P^l_{\phi_1}(t), E(t), a\big) - m^l\big(P^l_{\phi_2}(t), E(t), a\big)\big)\hat{u}^l_2(t,a)\hat{u}^l(t,a)\, da\, dt, \\ (\lambda - C_{\nu^f}) \displaystyle\int_{\Omega^f} \big(\hat{u}^f(t,a)\big)^2 \, da\, dt \leqslant \frac{1}{2} \int_0^T \nu^f\big(E(t),0\big)\big(\hat{u}^f(t,0)\big)^2 \, dt, \\ (\lambda - C_{\nu^m}) \displaystyle\int_{\Omega^m} \big(\hat{u}^m(t,a)\big)^2 \, da\, dt \leqslant \frac{1}{2} \int_0^T \nu^m\big(E(t),0\big)\big(\hat{u}^m(t,0)\big)^2 \, dt, \end{cases} \tag{2.11}$$

where the time-integrals over the domain $[0, T]$ are also equal, in view of the boundary conditions in (2.9), to the following equations,

$$\frac{1}{2}\int_0^T \nu^e\big(E(t),0\big)\big(\hat{u}^e(t,0)\big)^2 \, dt = \frac{1}{2}\int_0^T \frac{1}{\nu^e(E(t),0)} \left(\int_0^{L^f} \beta^f\big(P^f_1\big)\hat{u}^f(t,s)\, ds + \int_0^{L^f} \big(\beta^f\big(P^f_1\big) - \beta^f\big(P^f_2\big)\big)\hat{u}^f_2(t,s)\, ds \right)^2 dt,$$

$$\frac{1}{2}\int_0^T \nu^l\big(E(t),0\big)\big(\hat{u}^l(t,0)\big)^2 \, dt = \frac{1}{2}\int_0^T \frac{1}{\nu^l(E(t),0)} \left(\int_0^{L^e} \beta^e\big(E(t),s\big)\hat{u}^e(t,s)\, ds \right)^2 dt,$$

$$\frac{1}{2}\int_0^T \nu^f\big(E(t),0\big)\big(\hat{u}^f(t,0)\big)^2 \, dt = \frac{1}{2}\int_0^T \frac{\tau^2}{\nu^f(E(t),0)} \left(\int_0^{L^l} \beta^l\big(E(t),s\big)\phi(t,s)\, ds \right)^2 dt,$$

$$\frac{1}{2}\int_0^T \nu^m\big(E(t),0\big)\big(\hat{u}^m(t,0)\big)^2 \, dt = \frac{1}{2}\int_0^T \frac{(1-\tau)^2}{\nu^m(E(t),0)} \left(\int_0^{L^l} \beta^l\big(E(t),s\big)\phi(t,s)\, ds \right)^2 dt.$$

Consider now the second inequality of (2.11) and the two integrals on the right-hand side. We apply the Cauchy–Schwartz inequality to the first integral and Young's inequality to the second one, and we see that

$$\begin{aligned} (\lambda - C_{\nu^l}) \int_{\Omega^l} \big(\hat{u}^l(t,a)\big)^2 \, da\, dt \leqslant{} & \frac{1}{2}\int_0^T \frac{1}{\nu^l(E(t),0)} \int_0^{L^e} \big(\beta^e\big(E(t),s\big)\big)^2 ds \int_0^{L^e} \big(\hat{u}^e(t,s)\big)^2 \, ds\, dt \\ & + \int_{\Omega^l} \frac{\epsilon}{2}\big(m^l\big(P^l_{\phi_1}(t), E(t), a\big) - m^l\big(P^l_{\phi_2}(t), E(t), a\big)\big)^2 \, da\, dt \\ & + \int_{\Omega^l} \frac{1}{2\epsilon}\big(\hat{u}^l_2(t,a)\hat{u}^l(t,a)\big)^2 \, da\, dt, \end{aligned}$$

where ϵ is a positive constant. Hypotheses (H1)–(H6) enable us to conclude that inequality (2.11) is equivalent to (2.12)

$$\begin{aligned} \left(\lambda - C_{\nu^l} - \frac{\|\hat{u}^l_2\|^2_{L^\infty}}{2\epsilon}\right) \int_{\Omega^l} \big(\hat{u}^l(t,a)\big)^2 \, da\, dt \leqslant{} & \frac{L^e \|\beta^e\|^2_{L^\infty(\Omega^e)}}{2\underline{\nu}^l} \int_{\Omega^e} \big(\hat{u}^e\big)^2(t,s)\, ds\, dt \\ & + \frac{\epsilon}{2}\big(m^l_N L^l\big)^2 \int_{\Omega^l} (\phi_1 - \phi_2)^2(t,s)\, ds\, dt, \end{aligned} \tag{2.12}$$

which depends on the $L^2(\Omega^e)$-norm of the egg stage density. We estimate this norm from the first inequality of (2.11), by expanding the square of the sum in the right-hand side of (2.12) and by applying the Cauchy–Schwartz inequality to each of the terms on the right side, to finally get the following:

$$\begin{aligned}(\lambda - C_{v^e})\int_{\Omega^e}\big(\hat{u}^e(t,a)\big)^2\,da\,dt \leqslant{}& \frac{1}{2}\int_0^T \frac{1}{v^e(E(t),0)}\int_0^{L^f}\big(\beta^f\big(P_1^f\big)\big)^2\,ds\int_0^{L^f}\big(\hat{u}^f(t,s)\big)^2\,ds\\ &+\frac{1}{2}\int_0^T \frac{1}{v^e(E(t),0)}\int_0^{L^f}\big(\beta^f\big(P_1^f\big)-\beta^f\big(P_2^f\big)\big)^2\,ds\int_0^{L^f}\big(\hat{u}_2^f(t,s)\big)^2\,ds\,dt\\ &+\int_0^T \frac{1}{v^e(E(t),0)}\int_0^{L^f}\beta^f\big(P_1^f\big)\hat{u}^f(t,s)\,ds\int_0^{L^f}\big(\beta^f\big(P_1^f\big)-\beta^f\big(P_2^f\big)\big)\hat{u}_2^f(t,s)\,ds\,dt,\end{aligned}$$

or equivalently, by using hypotheses (H1)–(H6), to inequality (2.13),

$$(\lambda - C_{v^e})\int_{\Omega^e}\big(\hat{u}^e(t,a)\big)^2\,da\,dt \leqslant D_1\int_{\Omega^f}\big(\hat{u}^f(t,s)\big)^2\,ds, \tag{2.13}$$

where D_1 is a positive constant equal to

$$D_1 = \frac{L^f\|\beta^f\|^2_{L^\infty}}{2\underline{v}^e} + \frac{(L^f\beta_K^f)^2\|\hat{u}_2^f\|^2_{L^\infty}}{2\underline{v}^e} + \frac{L^f\|\beta_1^f\|^2_{L^\infty}\|\hat{u}_2^f\|_{L^\infty}\beta_K^f}{\underline{v}^e}.$$

The third inequality of (2.11) is used to estimate the norm in $L^2(\Omega^f)$ of the female density, by using the same method used to get (2.12) and (2.13), that gives

$$(\lambda - C_{v^f})\int_{\Omega^f}\big(\hat{u}^f(t,a)\big)^2\,da\,dt \leqslant \frac{L^l\tau^2\|\beta^l\|^2_{L^\infty(\Omega^l)}}{2\underline{v}^f}\int_{\Omega^l}\big(\phi(t,s)\big)^2\,ds. \tag{2.14}$$

Now, we use (2.14) to rewrite (2.13) in the form

$$(\lambda - C_{v^f})(\lambda - C_{v^e})\int_{\Omega^e}\big(\hat{u}^e(t,a)\big)^2\,da\,dt \leqslant D_1\frac{L^l\tau^2\|\beta^l\|^2_{L^\infty(\Omega^l)}}{2\underline{v}^f}\int_{\Omega^l}\big(\phi(t,s)\big)^2\,ds,$$

and we use this last inequality in (2.12) to conclude that

$$\begin{aligned}&\left(\lambda - C_{v^l} - \frac{\|\hat{u}_2^l\|^2_{L^\infty}}{2\epsilon}\right)(\lambda - C_{v^e})(\lambda - C_{v^f})\int_{\Omega^l}\big(\hat{u}^l(t,a)\big)^2\,da\,dt\\ &\quad\leqslant\left(D + (\lambda - C_{v^e})(\lambda - C_{v^f})\frac{\epsilon}{2}\big(m_N^lL^l\big)^2\right)\int_{\Omega^l}(\phi)^2(t,s)\,ds\,dt,\end{aligned}$$

where D is a positive constant given by

$$D = D_1\frac{L^l\tau^2\|\beta^l\|^2_{L^\infty(\Omega^l)}}{2\underline{v}^f}\,\frac{L^e\|\beta^e\|^2_{L^\infty(\Omega^e)}}{2\underline{v}^l}.$$

Let c be the constant defined by

$$c = \frac{(D + (\lambda - C_{v^e})(\lambda - C_{v^f})\frac{\epsilon}{2}(m_N^lL^l)^2)}{(\lambda - C_{v^l} - \frac{\|\hat{u}_2^l\|^2_{L^\infty}}{2\epsilon})(\lambda - C_{v^e})(\lambda - C_{v^f})}.$$

For fixed ϵ and λ chosen sufficiently large to satisfy the condition

$$D + (\lambda - C_{v^e})(\lambda - C_{v^f})\frac{\epsilon}{2}\big(m_N^lL^l\big)^2 < \left(\lambda - C_{v^l} - \frac{\|\hat{u}_2^l\|^2_{L^\infty}}{2\epsilon}\right)(\lambda - C_{v^e})(\lambda - C_{v^f}),$$

c lies in the interval $[0,1]$ and $\wedge$ is a contractive operator, as claimed. $\square$

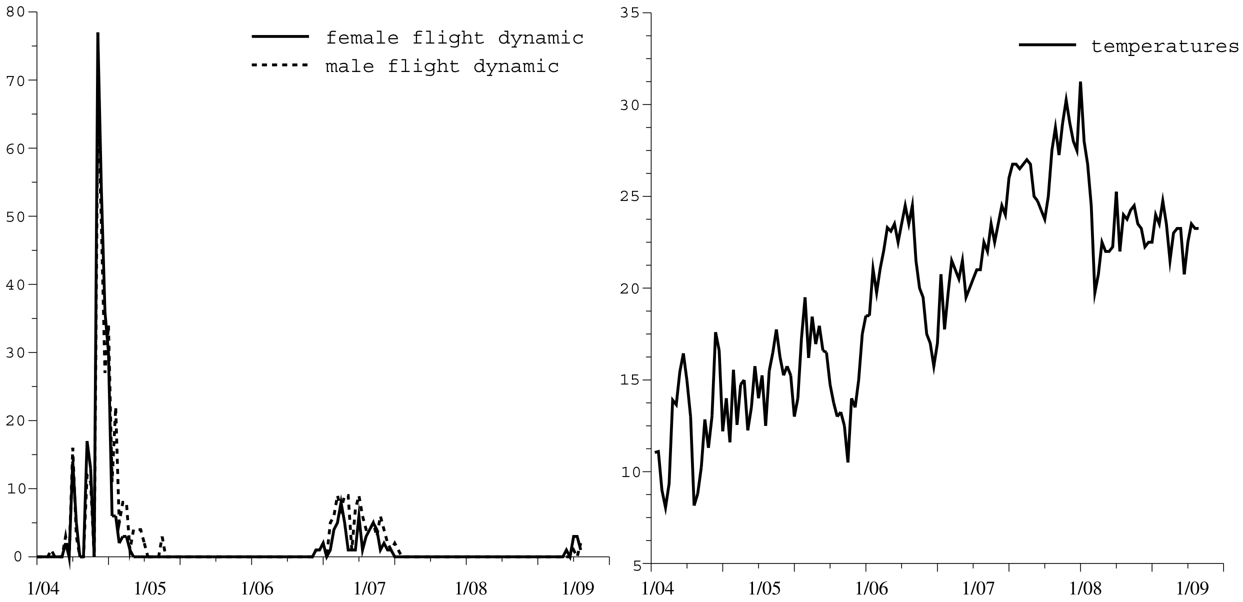

Fig. 1. Chavent's field experimental data from April to September 1983. Left: Female (solid) and male (dash dot) flight dynamics. Right: Daily mean temperatures.

3. Simulations

In this section, we apply LBM on a set of field experimental data and we compare these simulations with the measured population dynamics. The two first subsections are devoted to the presentation of the data, the definition of the model's demographic functions and the methods developed to produce simulations. In the last one, we present the results and we discuss them.

3.1. Material and methods

Field experimental data

In the literature, one can find very few field experimental data related to EGVM. We go back in 1983 to find Chavent's data [6] who measured adult flight dynamics in the vineyard during the whole season. He used individuals harvested from the vineyard to get the population dynamics. The advantage of his data is one knows the initial population size and its evolution in time unlike when using sexual and food traps that do not give these information, though they are very helpful for model simulations.

The data are numbers of emerging male and female moths per day of the first and second insect generations, and also the daily mean temperature (Fig. 1). Individuals were harvested at the pupa stage during winter for the first generation and during spring for the second one. These two samples are a representation of the natural population taken at two different times, meaning that the individuals of the second generation are not the descendants of the first one. The first dynamics (first peak), obtained with 660 winter pupa, starts April 5th and ends May 5th. The second one starts June 18th with 600 spring pupa harvested between June 6th and 22th and ends July 12th. The temperature is increasing during the experiment except at the end of May. These two samples are followed in a cage situated in a vineyard of the Southeast of France, consequently individuals are not affected by predators.

Unfortunately, these data do not give information about daily mean hygrometry, nor about grape variety of the vineyard. We then neglect these two factors in the simulations, and assume that the temperature is the only important factor to explain the data.

Growth functions $v^k(E(t), a)$, for $k = e, l, f, m$

In 1998, Brière measured mean development time of eggs, 5 larval stages and pupa at constant temperature [4]. The growth rate is defined as the reciprocal of the mean development time. Brière then deduced from his data the growth rate of eggs, larval stages and pupa at constant climatic conditions. To describe his data he tested several mathematical equations [4] and concluded that Logan and his equations [4,8] are the best fit. As the number of unknown parameters is smaller in Brière's equation, we use it to define our functions v^e and v^l in the form

$$v^k\big(E(t), a\big) = b^k T\big(T - T_0^k\big)\sqrt{\big(T_l^k - T\big)},$$

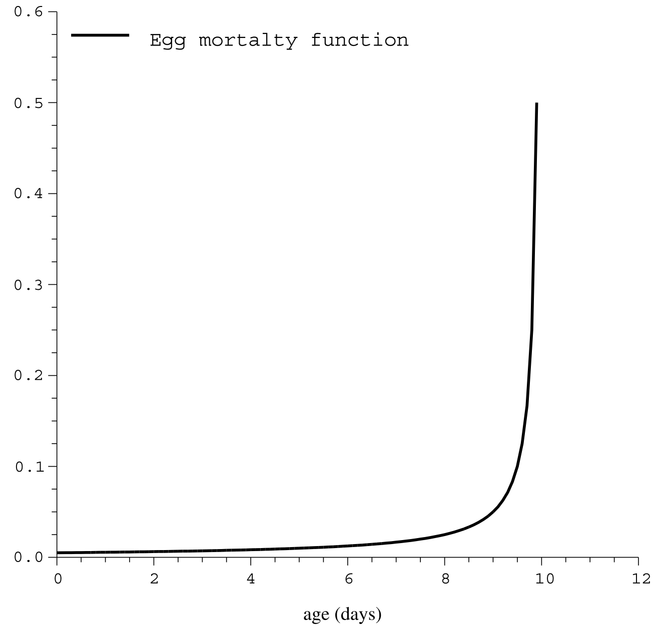

Fig. 2. Egg mortality function with respect to the age variable.

where T_0^k and T_l^k are the temperatures of low and maximal development for the k-developmental stage and b^k empirical constants, for $k = e, l$.

The mean development time of adults was not measured with respect to the temperature as done for eggs and larvae; Therefore, we define the adult growth function as constant and we set it equal to 1.

Mortality functions $m^k(E(t), a)$, for k equals to e, f, m

The mortality of a population is actually the combination of a natural mortality and a mortality caused by the environment. In field conditions, it is very difficult to measure the mortality rate of a population. For EGVM, the morality rates are measured in laboratory conditions with respect to some values of temperature [15], of humidity [1,15] and grape variety [10]. Globally, the mortality is very low for each developmental stage, around 2%, even for extreme negative or positive temperatures, without considering predators, parasitoids and dryness. We then assume that the mortality is, for each stage, an increasing function of age. Fig. 2 represents the egg mortality function where the maximum age is set to 10 days.

Larval mortality function $m^l(P^l(t), E(t), a)$

The larval mortality function is slightly different than the one defined above because it models the competition between larvae. We assume that the larval mortality can reach the value of 50% as soon as there are more than 10 larvae per bunch. Considering that the average number of bunches per parcel is around 6000 in French wine agriculture, this hypothesis implies that the larval population size cannot reach the number of more than 60 000 individuals. The function is then defined by the following equation,

$$m^l\big(P^l(t), E(t), a\big) = \frac{c}{L^l - a} e^{\frac{P^l(t)}{60\,000} - 1},$$

where c is a positive constant.

Transition functions $\beta^k(E(t), a)$, for $k = e, l$

According to our observations of the hatching and adult flight dynamics at constant temperature in the range [20 °C, 22 °C], the mean development time of an egg cohort is 6 days with a variation of around 3 days [1] whereas it is of 25 days with a variation of 20 days for a larval cohort [16]. The distribution around the mean is uniform and symmetric. We then define the functions $\beta^e(E(t), a)$ and $\beta^l(E(t), a)$ as Gaussian functions in the age variable for all environmental conditions with the means and variances set to 7 and 0.55, 26 and 0.35 respectively.

Birth function $\beta^f(P^f(t), P^m(t), E(t), a)$

Our hypotheses are based on Torres-Vila's results summarized in the paper [21]. He measures the dependence of the egg laying dynamics of females with respect to their age and their diet. The dynamics, for females growing on immature bunches, is represented by a decreasing curve with maximum value 30 and reaching the minimum value at around 6 days.

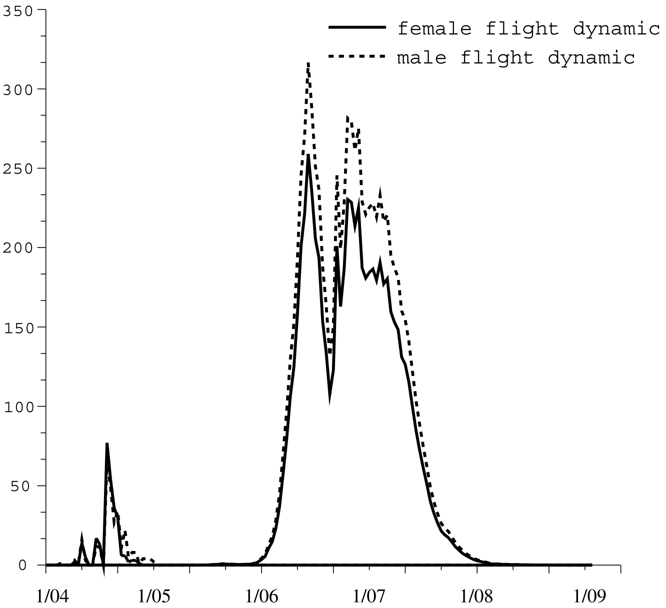

Fig. 3. Female (solid) and male (dash dot) flight dynamics from April to September 1983. These curves are the results of LBM.

He also proves that the fecundity rate is density-dependent and decreases as soon as the female population size is 8 time bigger than the male population size. According to these results, we define the birth function as follows

$$\beta^f\big(P^f(t), P^m(t), E(t), a\big) = \begin{cases} -5a+30 & \text{if } P^f(t) \leqslant 8P^m(t), \\ (-5a+30)e^{-(P^f(t)-8P^m(t))} & \text{if } P^f(t) > 8P^m(t). \end{cases}$$

3.2. Method

The model (2.1)–(2.3) is solved by a numerical method based on a Finite Volume scheme presented in the paper [17]. This method was chosen for its stability properties and its convergence, which is satisfactory for our study.

The model is initialized from the boundary conditions (2.2) of the adult stage with the first generation dynamics of Chavent's data. The initial conditions (2.3) are set to 0. The objective is then to simulate the second generation dynamics with LBM and to compare the model's predictions with Chavent's data. The comparison will be focused on the date of the first occurrence of moths and on the length of the adult flight dynamics. Chavent's data represents only a sample of the population dynamics, making a comparison with the simulated population size meaningless.

In the following simulations the maximal ages for each stage are chosen as follows:

$$L^e = 10; \qquad L^l = 35; \qquad L^f = L^m = 15,$$

and are given in days. The sex-ratio is 45/55 (% female/% male) that is consistent with the results of the papers [19,20]. The constants b^k, T_0^k and T_l^k for $k = e, l$ used in the growth functions, and c used in the mortality functions are

$$b^e = 1.710^{-4}, \qquad b^l = 3.510^{-5}, \qquad T_0^e = 10.55, \qquad T_0^l = 12.2, \qquad T_l^e = 34, \qquad T_l^l = 34.2, \qquad c = 0.05.$$

3.3. Results and discussion

Fig. 3 shows the LBM simulations of the first and second generations of female (solid line) and male (dash dot line) populations.

The emerging moths period of the second generation predicted by LBM coincides with Chavent's data and occurs two months after the first generation which is consistent with the insect biology. The decline of emerging moths number at the end of June in Chavent's data is also predicted by our model. However, the estimation of the beginning and the end of this period are, respectively, 2 weeks earlier and 2 weeks later than those measured by Chavent. The number of adults estimated by LBM for the second insect generation varies between a maximum of 300 to a minimum of 150 individuals for the male population and, 250 to 150 individuals for the female population. The population size is then 10 to 30 times bigger than the size of the sample followed by Chavent explaining partly the variability of the emerging dates and then a longer predictive dynamics.

In this simple example of model application, we use parameters (mortality, birth, growth and transition functions) defined from experimental results obtained under constant environmental conditions whereas LBM is really applied to predict

EGVM dynamics in a vineyard where the temperature fluctuates. Also, we neglect the environmental factors such as air hygrometry and grape variety in LBM simulations because of a lack of data. By considering them, the model could give a best estimate of the duration of the second adult flight dynamics (Fig. 3). To improve these simulations, we then propose to estimate all LBM parameters from experimental data. Laboratory data could be used as a first step. Indeed, in such experimental conditions, several factors are constant in time and biological characteristics neglected, leading, from a mathematical point of view, to make some simplifications in the model. The next steps are to define the parameters with mathematical equations considering all environmental factors and then validate them by running simulations as we did in this section.

4. Conclusion

Nowadays, the tools used to predict the appearance of the European Grapevine Moth (EGVM) in a vineyard are monitoring traps (pheromone for moths or food traps for females), and visual counting of eggs and larvae at each generation. These tools help wine makers to know whether or not moths exist at a given moment. From this information, they deduce the egg laying and hatching periods. It is easy to understand that such techniques have several drawbacks. Indeed, wine makers do not have information on the real moth population size and on the age of the moths. Moreover, these tools do not highlight the appearance of eggs and larvae in the vineyard. Therefore, a mathematical model could be a helpful tool to generate an approximation of these missing information. Its main objective will be to predict in time and stage the pest population size within a given vineyard.

The *Lobesia botrana* model (LBM) developed in this paper structures the population into four stages which are egg, larval, female and male adults. It models also the physiological age of individuals for each stages. Such a model structure leads to a better understanding not only of the population size fluctuations but also of the egg laying behavior or the dynamic of vine damages by young larvae, for example.

Creating a realistic model is only possible if we consider the main environmental factors. Our model consider three of them namely the temperature, the air hygrometry and the grape variety. Previous works focused more on the effect of the temperature, neglecting the two other factors. However, recent papers put forward evidence that they modify several life history traits like for example the population fitness, the growth speed of larvae, the choice of the mate, the fecundity and egg survival [9–13,19,20]. All this contributes to growth population fluctuations.

To accurately predict the “population peaks” of each stage, it is natural to consider physiological characteristics of this pest in the model. As a consequence, we use partial differential equations to describe the aging of our sub-populations. Also, the growth and the transition functions from one stage to the next are age-dependent in order to increase growth variations inside a cohort. To sum up, the model proposed in this paper is, for two reasons, unique. First, it describes the EGVM population dynamics with a hyperbolic system and, secondly, the model takes into account a great deal of biological information.

LBM offers a very good description of EGVM’s life cycle. However to model more sub-populations such as black egg stage or the 5 larval stages and be applied to other insect populations with similar life cycles, our model could be generalized by replacing the larval equation of the system (2.1) by

$$\begin{cases} \dfrac{\partial}{\partial t}u^k(t,a)+\dfrac{\partial}{\partial a}\big[v^k\big(E(t),a\big)u^k(t,a)\big]=-m^k\big(P^k(t),E(t),a\big)u^k(t,a)-\beta^k\big(E(t),a\big)u^k(t,a),\\ \dfrac{\partial}{\partial t}u^{k+1}(t,a)+\dfrac{\partial}{\partial a}\big[v^{k+1}\big(E(t),a\big)u^{k+1}(t,a)\big]=-m^{k+1}\big(P^{k+1}(t),E(t),a\big)u^{k+1}(t,a)-\beta^{k+1}\big(E(t),a\big)u^{k+1}(t,a),\end{cases}$$

where k refers to the stage after the newborn one. The boundary conditions of the larval and adult stages of (2.2) are then given by

$$\begin{cases} v^k\big(E(t),0\big)u^k(t,0)=\displaystyle\int_0^{L^e}\beta^e\big(E(t),s\big)u^e(t,s)\,ds,\\ v^{k+1}\big(E(t),0\big)u^{k+1}(t,0)=\displaystyle\int_0^{L^k}\beta^k\big(E(t),s\big)u^k(t,s)\,ds,\\ \dots,\\ v^f\big(E(t),0\big)u^f(t,0)=\displaystyle\int_0^{L^l}\tau\beta^{k+n}\big(E(t),s\big)u^{k+n}(t,s)\,ds,\\ v^m\big(E(t),0\big)u^m(t,0)=\displaystyle\int_0^{L^l}(1-\tau)\beta^{k+n}\big(E(t),s\big)u^{k+n}(t,s)\,ds,\end{cases}$$

where n is the number of stages added to structure the population and $k+n$ refers to the stage just before the adult one. The initial conditions of the added equations are defined by

$$\begin{cases} u^k(0,a) = u_0^k(a), \quad a \in [0, L^k], \\ \dots, \\ u^{k+n}(0,a) = u_0^{k+n}(a), \quad a \in [0, L^{k+n}]. \end{cases}$$

The proof of existence and uniqueness of solution for this general model is given in this paper for $k = l$ and $n = 0$ and, but it holds just the same for $k \neq l$ and $n > 0$.

In the last section, we compare the model predictions with field experimental data. The simulations are not identical to the data because of the lack of information about the data but also about the relation between insect biology and our modeled environmental factors. We think we should first estimate model parameters with data obtained in a control environment to accurately define and understand this relation, and then validate the model with such field data.

Acknowledgments

This work was accomplished during the PhD of Dr. Picart which was funded by a grant from Région Aquitaine and the French National Institute for Research in Computer Science and Control (www.inria.fr). We thank Prof. Milner for helping us in the writing of this paper.

References

[1] O. Auroy, Estimation des traits d'histoire de vie de l'Eudémis de la vigne (*Lobesia botrana* Den. et Schiff.) en vue d'une utilisation dans un modèle mathématique, Mémoire de fin d'études, d'ingénieur de l'ENITA de Bordeaux, 2006.
[2] H.T. Banks, L.K. Potter, Probabilistic methods for addressing uncertainty and variability in biological models: application to a toxicokinetic model, Math. Biosci. 192 (2004) 193–225.
[3] J. Baumgartner, P. Baronio, Modello fenologico di volo di Lobesia botrana Den. et Schiff. (Lep. Tortricidae) relativo alla situazione ambientale della Emilia Romagna, Bollettino dell'Istituto di Entomologia "Guido Grandi" 43 (1988) 157–170.
[4] J.F. Brière, Analyse mathématique et numérique d'un modèle spatio-temporel de la dynamique d'un ravageur de la vigne : *Lobesia botrana* (Eudémis), Thèse en Mathématiques et Informatique, Université Bordeaux 1, 1998.
[5] A. Calsina, J. Saldana, A model of physiologically structured population dynamics with a nonlinear individual growth rate, J. Math. Biol. 33 (1995) 335–364.
[6] F. Chavent, Etude de la dynamique des populations d'Eudémis de la vigne (Lobesia Botrana Den. et Schiff.) : Adaptation d'un modèle d'évolution aux conditions climatiques de la Provence.
[7] R.M. Gurtin, R.C. MacCamy, Non-linear age-dependent population dynamics, Arch. Ration. Mech. Anal. 3 (1974) 281–300.
[8] J.A. Logan, D.J. Wollkind, S.C. Hoyt, L.K. Tanigoshi, An analytic model for description of temperature dependent rate phenomena in arthropods, Environ. Entomol. 5 (1976) 1133–1140.
[9] J. Moreau, X. Arruego, B. Benrey, D. Thiéry, Differences in nutritional quality of parts of Vitis vinifera berries affect fitness of the European grapevine moth, Entomol. Exp. Appl. 119 (2006) 93–99.
[10] J. Moreau, B. Benrey, D. Thiéry, Grape variety affects larval performance and also female reproductive performance of the European grapevine moth Lobesia botrana (Lepidoptera: Tortricidae), Bull. Entomol. Res. 96 (2006) 205–212.
[11] J. Moreau, D. Thiéry, J.P. Troussard, B. Benrey, Grape variety affects female but also male reproductive success in wild European grapevine moth, Ecol. Entomol. 332 (2007) 747–753.
[12] J. Moreau, J. Rahmé, B. Benrey, D. Thiéry, Larval host-plant origin modifies the adult oviposition preference of the European grapevine moth Lobesia botrana, Naturwissenschaften 95 (2008) 317–324.
[13] J. Moreau, A. Richard, B. Benrey, D. Thiéry, The influence of plant cultivar of the grapevine moth Lobesia botrana on the life history traits of an egg parasitoïd, Biol. Control 50 (2009) 117–122.
[14] J.D. Murray, Mathematical Biology I: An Introduction, third ed., Springer-Verlag, Berlin, 2002.
[15] L. Oustry, Influence des facteurs abiotiques et trophiques sur le développement de l'Eudémis de la vigne (*Lobesia botrana* Den. et Schiff.) application à la modélisation, Mémoire de fin d'étude ENITA Bordeaux, 1991.
[16] D. Picart, Modélisation et estimation des paramètres liés au succès reproducteur d'un ravageur de la vigne (Lobesia botrana Den. et Schiff.), PhD thesis No. 3772, University of Bordeaux, 2009.
[17] D. Picart, B. Ainseba, Parameter identification in multistage population dynamics model, Nonlinear Anal. Ser. B: Real World Appl., submitted for publication.
[18] J.W. Sinko, W. Streifer, A new model for age-size structure of a population, Ecology 48 (1967) 910–918.
[19] D. Thiéry, J. Moreau, Relative performance of European grapevine moth (Lobesia botrana) on grapes and other hosts, Oecologia 143 (2005) 548–557.
[20] D. Thiéry, Les tordeuses nuisibles à la vigne, in: S. Kreiter (Ed.), Ravageurs de la vigne, Féret, Bordeaux, France, 2008, pp. 214–246.
[21] L.M. Torres-Vila, M.C. Rodrihuez-Molina, R. Roehrich, J. Stockel, Vine phenological stage during larval feeding affects male and female reproductive output of Lobesia botrana (Lepidoptera: Tortricidae), Bull. Entomol. Res. 89 (1999) 549–556.
[22] J. Touzeau, Etude des principaux paramètres biotiques et abiotiques nécessaire à l'établissement d'un modèle d'évolution de l'Eudémis de la vigne (*Lobesia Botrana* Schiff.) pour la région Midi-Pyrénées, 1979.